



ARTICLE OPEN

Dasatinib and quercetin senolytic treatment delays early onset intervertebral disc degeneration in SM/J mice

Emanuel J. Novais^{1,2,3,4,5}, Olivia K. Ottone^{1,2}, Sanjana Jagannath¹, Esther Jesutofunmi Akande¹, Ruteja A. Barve⁶ and Makarand V. Risbud^{1,2}✉

Genetic background is a major determinant of disc degeneration, a leading cause of chronic back pain and disability. Herein, we demonstrate that premature disc cell senescence contributes to early-onset degeneration in SM/J mice and test two systemic senotherapeutic strategies to mitigate it: Navitoclax (Nav.) and a cocktail of Dasatinib and Quercetin (DQ). While Nav. treatment did not improve severe degeneration in SM/J mice or senescence status, DQ-treated mice showed lower grades of degeneration and a decreased abundance of senescence markers, including p19ARF, p21, and the senescence-associated secretory phenotype (SASP). DQ improved disc cell viability and phenotype retention and retarded fibrosis of the nucleus pulposus tissue. Transcriptomic analysis revealed tissue-specific effects of the treatment, with cell cycle regulation and JNK signaling being commonly affected across different tissue types. A comparison of SM/J data with DQ-mediated aging-dependent amelioration of disc degeneration in C57BL/6 N mice identified *Junb* and *Zfp361* signaling as shared DQ targets in the mouse disc. Notably, the in vitro inhibition studies of the JUN pathway in human degenerated NP cells mimicked the benefits of DQ, namely, a reduction in senescence and SASP. This study reinforces the efficacy of senolytic treatment in ameliorating local senescence and intervertebral disc fibrosis.

Bone Research (2026)14:42

; <https://doi.org/10.1038/s41413-026-00526-4>

INTRODUCTION

Low back pain (LBP) and neck pain rank among the top causes of years lived with disability.¹ Though the etiology of LBP is multifactorial, patients with intervertebral disc degeneration are three times more susceptible to LBP.² The intervertebral disc sandwiched between the adjacent vertebrae confers spinal flexibility and accommodates loading.³ This ability results from the interaction of the disc compartments: the central, glycosaminoglycan-rich nucleus pulposus (NP); the circumferential, annulus fibrosus (AF), comprised of highly organized collagen fibrils; and endplates (EP), which consist of a thin layer of hyaline cartilage and a subchondral bone plate.⁴ Each compartment is distinguished by its extracellular matrix, which maintains largely non-proliferative cells adapted to accommodate the physiological avascular and hypoxic conditions of the disc.^{5,6} Degeneration affects each disc compartment, and abnormal function of any of them influences the degenerative cascade of the others.⁷ Broadly, the degenerative process is characterized by altered extracellular matrix (ECM) organization and composition,⁸ loss of biomechanical properties,⁹ increased inflammatory mediators and catabolic processes, changes in cell phenotype, cell death,¹⁰ and senescence.^{11,12}

Among many factors contributing to disc degeneration, genetic predisposition is one of the major contributors to the disease process.¹³ Battié et al. demonstrated that genetics is the top predisposing factor to disc degeneration, followed by aging and loading in humans.¹⁴ Many studies have described a correlation

between the disease and several single-nucleotide polymorphisms related to extracellular matrix,¹⁵ matrix catabolism,¹⁶ inflammation,¹⁷ and cell signaling.¹⁸ More recently, we and others have shown that the genetic background governs the susceptibility to disc degeneration and the progression into specific disease sub-phenotypes, including fibrosis, ectopic calcification and herniation in mice.^{19–21}

Mechanistic studies of disc degeneration have been hindered by the need for suitable animal models that recapitulate human pathology without the use of genetic manipulation or injury. Recent studies have shown that the SM/J, an inbred mouse strain exhibiting poor healing ability, first described in the context of cartilage regeneration, undergoes spontaneous disc degeneration, replicating key molecular, phenotypic, and functional features, including aging-associated disc herniation and back pain in humans.^{9,19,21} The SM/J mouse is a promising model for studying disc degeneration due to its early onset, which recapitulates age-related phenotypes as early as 17 weeks.^{9,21} Additionally, these mice, unlike progeria models, present a comparable lifespan to other common models, such as C57BL/6.^{19,22} In other musculoskeletal fields, SM/J has been presented as a useful tool for advanced intercross line studies to identify quantitative trait loci associated with susceptibility to osteoarthritis and osteoporosis.^{23,24} However, the cellular mechanisms driving early-onset disc degeneration in SM/J mice remain relatively unexplored.

¹Department of Orthopaedic Surgery, Sidney Kimmel Medical College, Thomas Jefferson University, Philadelphia, USA; ²Graduate Program in Cell Biology and Regenerative Medicine, Jefferson College of Life Sciences, Thomas Jefferson University, Philadelphia, USA; ³Unidade Local de Saúde do Litoral Alentejano, Orthopedic Department, Santiago do Cacém, Portugal; ⁴Faculty of Medicine, Universidade Católica Portuguesa, Lisbon, Portugal; ⁵Center for Interdisciplinary Research in Health, Universidade Católica Portuguesa, Lisbon, Portugal and ⁶Department of Genetics, GenomeTechnology Access Centre at the McDonnell Genome Institute, Washington University, School of Medicine, St. Louis, MO, USA

Correspondence: Makarand V. Risbud (makarand.risbud@jefferson.edu)

These authors contributed equally: Emanuel J. Novais, Olivia K. Ottone

Received: 6 June 2025 Revised: 13 January 2026 Accepted: 11 February 2026

Published online: 14 April 2026

Several studies have demonstrated the role of senescence in intervertebral degeneration in humans and mice.^{10,11} Senescence is broadly characterized by cell cycle arrest, resistance to apoptosis, and the production of inflammatory and catabolic factors, collectively known as the senescence-associated secretory phenotype (SASP).²⁵ The increased expression of cell cycle inhibitors such as p21, p53, p16^{INK4a}, and p19^{ARF} across tissues is a hallmark of this cell stage.²⁶ This senescent cell state causes local fibrosis, loss of regenerative capacity, and, ultimately, tissue degeneration.²⁵ Genetic and natural aging models have demonstrated that targeting senescence can modulate the progression of disc disease and back pain.^{10,27,28} Similarly, using cultured human disc cells, Cherif et al. demonstrated that the effective clearance of senescent disc cells reduced inflammatory signaling following senolytic intervention²⁹; however, there is limited knowledge about the applicability and success of senolytic treatments in targeting different phenotypes of disc degeneration in vivo.

Senolytic therapies, which selectively induce apoptosis of senescent cells, have gained substantial traction in musculoskeletal pathologies since they were first described in 2015.³⁰ Several compounds, such as ABT-263 (Navitoclax, Nav.), which targets the BCL-2 pathway³¹; BCL-XL inhibitors like A1331852 and A1155463³²; flavonoids, including Quercetin, Fisetin, and Piperlongumine; and Src/tyrosine kinase inhibitors²⁶ are shown to successfully remove senescent cells. Among the senotherapeutic compounds being studied, the combination of Dasatinib (D) – a Src/tyrosine kinase inhibitor – and Quercetin (Q) – a natural flavonoid that binds to BCL-2 and modulates transcription factors, cell cycle proteins, pro- and anti-apoptotic proteins, growth factors, and protein kinases³³ – (DQ) has shown the most promising results, with low toxicity.¹² Accordingly, DQ was the first senolytic approach used in clinical trials, showing efficiency in clearing senescent cells in humans and improving and promoting physical function.^{34,35} In the context of disc degeneration, we have recently demonstrated that systemic treatment with a DQ cocktail can effectively reduce the age-associated senescence burden and disc degeneration in C57BL/6N (B6N) mice.³⁶

In this study, we demonstrate that early-onset, spontaneous disc degeneration in SM/J mice is associated with elevated senescence burden. Importantly, we determined the efficacy of systemic DQ and Nav. treatment in targeting senescence in the disc and alleviating the early onset of degenerative processes. Notably, our results show that DQ, but not Nav., reduces the severity of disc degeneration and the senescence burden by targeting the *Jun* and *Zfp3611* signaling pathways. This work further supports the potential of systemically delivered DQ to ameliorate the effects of early-onset, spontaneous disc degeneration and contribute to deciphering the mechanisms of senotherapeutic systems, which may support future clinical applications.

RESULTS

SM/J mice show a high senescence burden which coincides with the progression of disc degeneration

SM/J mice show early onset, spontaneous disc degeneration, recapitulating several salient features of human degeneration by the time animals are 17 weeks old.^{9,21} Considering the role of cellular senescence in intervertebral disc degeneration,^{10,11,12} we investigated the senescence status of SM/J discs at 4 weeks, prior to the conspicuous cell death in the NP compartment.⁹ Interestingly, 4-week-old SM/J caudal discs presented higher levels of senescence markers p19 (Fig. 1a–a”) and p21 (Fig. 1b–b”), compared to C57BL/6J (B6J) mice, which expresses these markers with aging, between 18–24 months.^{10,12} To investigate the contribution of cell senescence to progression of degeneration in SM/J mice, global transcriptomic analysis was conducted on 4- and 17-week-old NP and AF tissues, which showed distinct profiles at the both timepoints (Fig. 1c). To gain insight into the functional implications of these transcriptomic

changes, the CompBio analysis tool (<https://gtac-compbio-ex.wustl.edu>) was used to determine thematic associations among differentially expressed genes^{36,37} (full results in Supplementary File 1). Notably, analysis of upregulated DEGs in 17-week-old SM/J NP tissue showed enrichment for *Beta-galactoside Alpha-2,3-sialyltransferase Activity* and *EPH-Ephrin Signaling*, which have implications in cellular senescence and response to senolytic compounds, such as Dasatinib^{38,39} (Fig. 1d, Fig. S1A). In the AF transcriptome, signatures associated with *VEGF-A Complex*, *IL1*, and *Megakaryocytes in Obesity*, *Hypokalemic Alkalosis*, and *Negative Regulation of TORC2 Signaling* increased during degeneration, demonstrating several molecular hallmarks of disc degeneration (Fig. 1e, Fig. S1. B–B”). In line with these findings, downregulated themes in the NP enriched around several matrix and cell cycle-related themes, including *CDK1 phosphorylates condensing and Transcription of E2F Targets*, *Heparan Sulfate 2-O-sulfotransferase Activity*, and *TNFR1-induced NFkB signaling pathway* (Fig. 1f, Fig. S1C–C”). Similarly, the downregulated themes in the AF were enriched for processes such as *RUNX2 regulates osteoblast differentiation*, *Arp2/3 Complex Binding*, and *Sos-mediated nucleotide exchange of Ras* (Fig. 1g, Fig. S1D–D”).

To more precisely investigate the correlation between the disc degeneration process in SM/J model with established senescence signatures, concept-level assertion engine analysis was conducted on CompBio outputs for up- and downregulated concepts in NP and AF tissues, compared to the published *SenMayo* gene set,⁴⁰ revealing significant associations in both tissues. Cross-referencing the DEG gene lists from NP and AF against the *SenMayo* dataset revealed several shared genes (Supplementary File 1). Thus, we compared the overlapping biological themes and concepts between the *SenMayo* Murine gene and upregulated DEGs from SM/J and SPARC-KO mice (models of early disc degeneration with senescence),²⁸ and old B6 mice (aging and senescence-dependent disc degeneration)¹² (Fig. S2). Except for upregulated DEGs in BL6 AF, all models presented high concept and theme similarity with the *SenMayo* panel (Fig. S2). Specifically, at the thematic level, we identified “TNF and Lymphotoxin Signaling” commonly modulated in all 5 conditions, followed by “Tissue Inhibitor of Metalloproteinases (TIMP) associated ECM remodeling”, “VEGF-A/Angiogenesis related”, “JNK (c-Jun kinases) phosphorylation and activation mediated by activated human TAK1”, “Interleukin-3 Interleukin-5 and GM-CSF signaling”, “Prostaglandin E2 Receptor EP2 Subtype” and Galactosylation of collagen propeptide hydroxylysines by procollagen galactosyltransferases” presented in SM/J, SPARC and BL6 models (Fig. S2).

These findings suggest that cellular senescence contributes to the degeneration observed in SM/J mice, and therefore, we sought to intervene in this degenerative progression using senotherapeutics.

DQ treatment, but not Navitoclax, improves degenerative and senescence outcomes in SM/J mice

Previously reported successful outcomes of DQ treatment in aging B6N mice were dependent on the age when the treatment was initiated, showing the maximum efficiency when administered during the early stages of the disease process, suggesting a finite window for local cellular response and plasticity.¹² Accordingly, beginning at 4 weeks of age and continued until 17 weeks, SM/J mice received either a weekly treatment with a Dasatinib (5 mg/kg) (D) and Quercetin (50 mg/kg) (Q) combination (DQ) (Fig. 2a) or Navitoclax (Nav.) (40 mg/kg) (Fig. 2b) to target senescent cells and ameliorate disc degeneration. Histological analysis of discs showed increased tissue preservation, cellularity, and cell morphology, with better NP/AF compartment demarcation and fewer AF clefts relative to vehicle-treated control animals (CT) (Fig. 2a’–a”). Improvements to the disc architecture were observed in the DQ treatment cohort as early as 6–8 weeks (Fig. S3A–B”). Further, modified Thompson grading showed a reduction of approximately 25% in severely degenerated (grade 4) NP and AF tissues (Fig. 2a”).^{19,41} By contrast, Navitoclax-

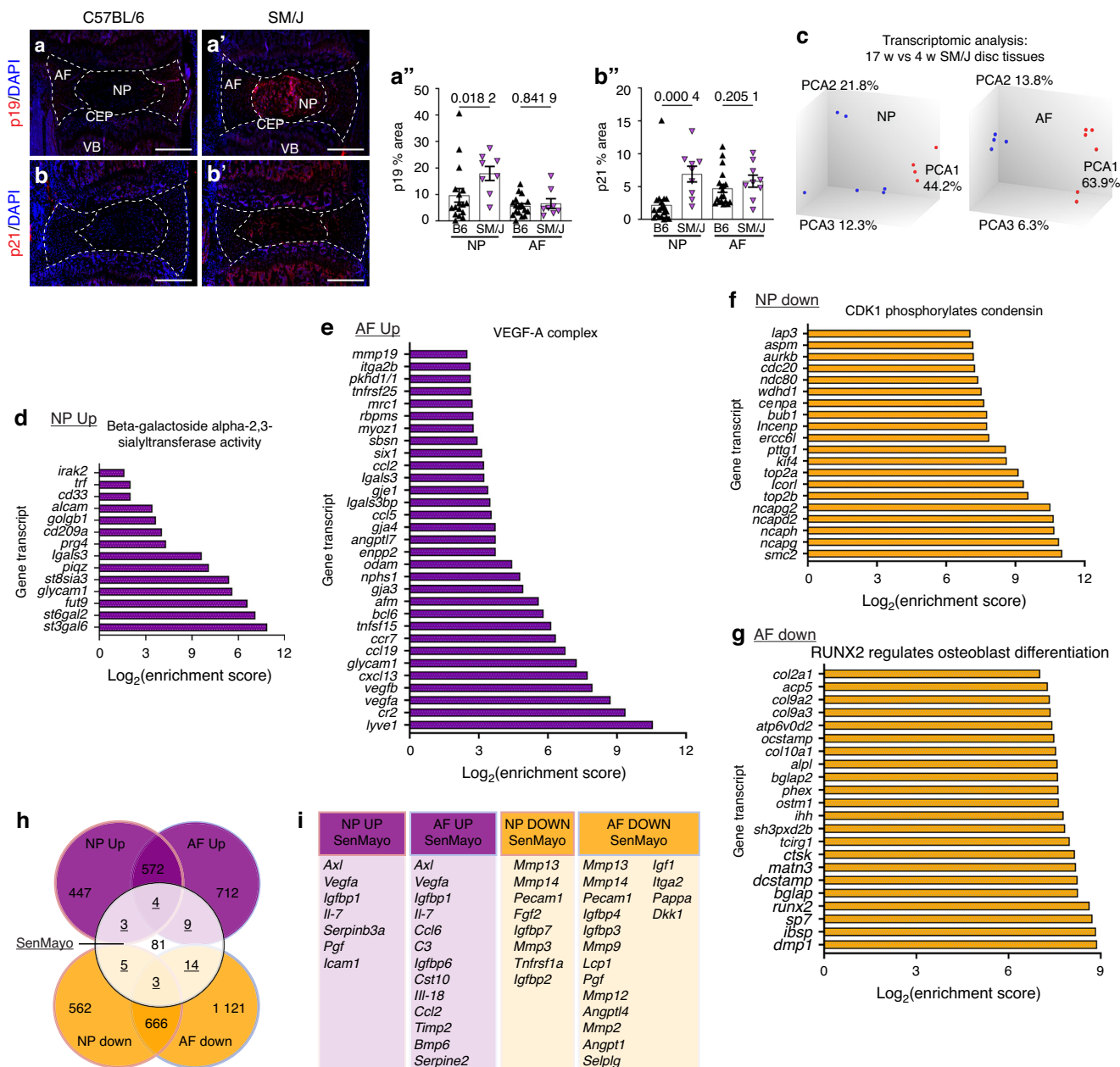


Fig. 1 Caudal discs of SM/J mice evidence early cellular senescence and a senescence signature during degeneration. At four weeks of age, SM/J mice have increased abundance of senescence markers in their caudal discs, evidenced by (a–a'') p19 and (b–b'') p21 abundance relative to age-matched B6J discs. c Microarray analysis of 4-week-old and 17-week-old SM/J NP and AF shows distinct clustering in both tissues between the two timepoints. Thematic analysis in CompBio of enriched concepts in 17-week-old NP tissues, compared to 4-week-old tissues shows: (d') *Beta-galactoside Alpha-2,3-sialyltransferase Activity* is an upregulated theme in the NP; (e) *VEGF-A Complex* is an upregulated theme in the AF; (f) *CDK1 Phosphorylates Condensin* is a downregulated theme in the NP; and (g) *RUNX2 Regulates Osteoblast Differentiation* is a downregulated theme in the AF. h Venn Diagram showing the gene-level overlap between SM/J tissue profiles and the *SenMayo* geneset, with the overlapping genes shown in (i). Data are shown as mean ± SD. Significance was determined using an unpaired *t*-test or Mann-Whitney test, as appropriate. $n_{C57BL/6J\ 4w} = 8$; $n_{SM/J\ 4w} = 5$; $n_{SM/J\ 17w} = 6$

treated mice did not demonstrate structural improvements in their discs, evidenced by histological analysis and modified Thompson scoring and disc tissue senescence status (Fig. 2b–b'' and S3F–H''). Accordingly, we focused on determining how DQ treatment modulates senescence and ameliorates disc degeneration in SM/J mice.

To better understand the cellular processes underlying the structural improvements to the disc, several indicators of cell senescence and SASP were evaluated at the tissue level, and the plasma cytokine profile was determined.^{25,27,41,42,43} In both NP

and AF tissues of DQ-treated mice, p19^{ARF} (p19) levels were reduced (Fig. 2c–c''), and p21 abundance was reduced in the AF (Fig. 2d–d''). These observations provided evidence of a reduced senescence burden in the disc tissues of SM/J mice by DQ treatment. Complementary analysis of SASP markers showed reduced IL-6 and MMP13 (Fig. 2e–g'') in the NP, reduced TGFβ (Fig. 2f–f''), without affect on IL-1β levels (Fig. 2h–h'') in the AF of DQ-treated mice. Notably, we observed an early senolytic effect of DQ treatment, characterized by a reduction in p19^{ARF} (p19) and p21 levels, despite no changes in IL-6 levels at 8 weeks of treatment

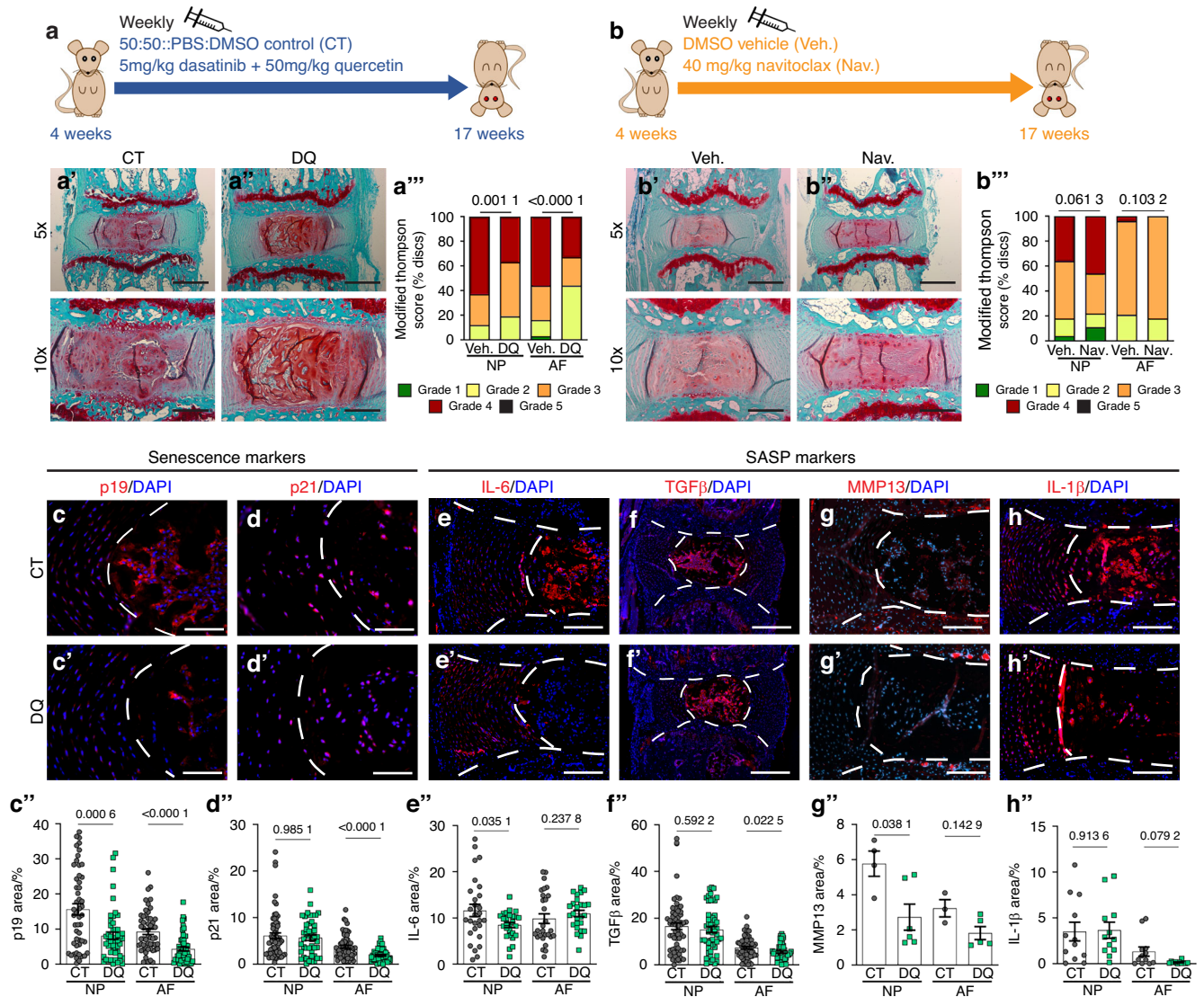


Fig. 2 DQ reduces caudal disc degeneration and senescence in SM/J mice. **a, b** Schematic showing study design: intraperitoneal injections of DQ, Nav, or a Vehicle control were administered once every week to mice starting at 4 weeks of age and ending at 17 weeks of age. **a'–a''** Safranin O/Fast Green/Hematoxylin staining evaluated with modified Thompson scoring shows DQ improves disc degeneration in SM/J mice. Images reflect the range of degenerative outcomes across treatment cohorts. **b'–b''** Safranin O/Fast Green/Hematoxylin staining evaluated with modified Thompson scoring shows Nav does not improve disc degeneration in SM/J mice. Quantitative immunohistochemistry shows reduced (**c–c''**) p19 (NP and AF) and (**d–d''**) p21 (AF only) in DQ-treated SM/J discs. SASP markers of (**e–e''**) TGF β , (**f–f''**) IL-6, (**g–g''**) MMP13, and (**h–h''**) IL-1 β indicate DQ mediates SASP in SM/J discs. Data are shown as mean \pm SD. Significance was determined using an unpaired *t*-test or Mann-Whitney test, as appropriate. Distribution statistics were determined using a χ^2 test. 17 weeks old ($n_{DQ} = 11$, 6 females + 5 males; $n_{CT} = 13$, 6 females + 7 males; $n_{Nav.} = 7$, $n_{Veh.} = 7$)

(Fig. S3C–E). As anticipated, Nav. treatment did not affect local senescence status after 17 weeks of treatment, supporting the histological findings (Fig. S3F–H''). These changes indicated a reduction in local inflammation and pro-fibrotic signaling with DQ treatment, suggesting that DQ effectively reduces the incidence and severity of disc degeneration in SM/J mice by mitigating cell senescence and SASP. ^{38,39,44–46}

To study the effect of DQ treatment on systemic cytokine levels, we measured several pro-inflammatory molecules in plasma. Notably, DQ mice showed decreased levels of proinflammatory proteins MIP-2 (Fig. S4A) and MCP-1 (Fig. S4B), with trends toward reduction in IP-10 (Fig. S4C) ($P = 0.056$ 4), TNF- α (Fig. S4D) ($P = 0.057$ 7), and IL-4 (Fig. S4E) ($P = 0.054$ 7). This response was selective, as we noted a lack of change in several other plasma cytokines in DQ-treated mice (Fig. S4F–R). These results showed

that DQ treatment mitigated tissue-level pro-inflammatory response and attenuated systemic inflammation in SM/J mice.

To further evaluate the systemic impact of DQ treatment on SM/J mice, the caudal vertebral bone was analyzed using micro-computed tomography (μ CT). Three-dimensional reconstructions of the caudal vertebrae (Fig. S5A, A') showed no changes in the vertebral length (Fig. S5B), disc height (Fig. S5C), or disc height index (Fig. S5D). In the trabecular bone, the bone volume fraction (BV/TV) (Fig. S5E), trabecular thickness (Tb. Th.) (Fig. S5F), and trabecular number (Tb. N.) (Fig. S5G) were unchanged, while the DQ-treated cohort evidenced a slight reduction in trabecular spacing (Tb. Sp.) (Fig. S5H). This change is unlikely to bear functional significance due to its small magnitude and the absence of change in other parameters. Evaluation of the cortical bone (Fig. S5I, I') showed DQ did not impact bone volume (BV)

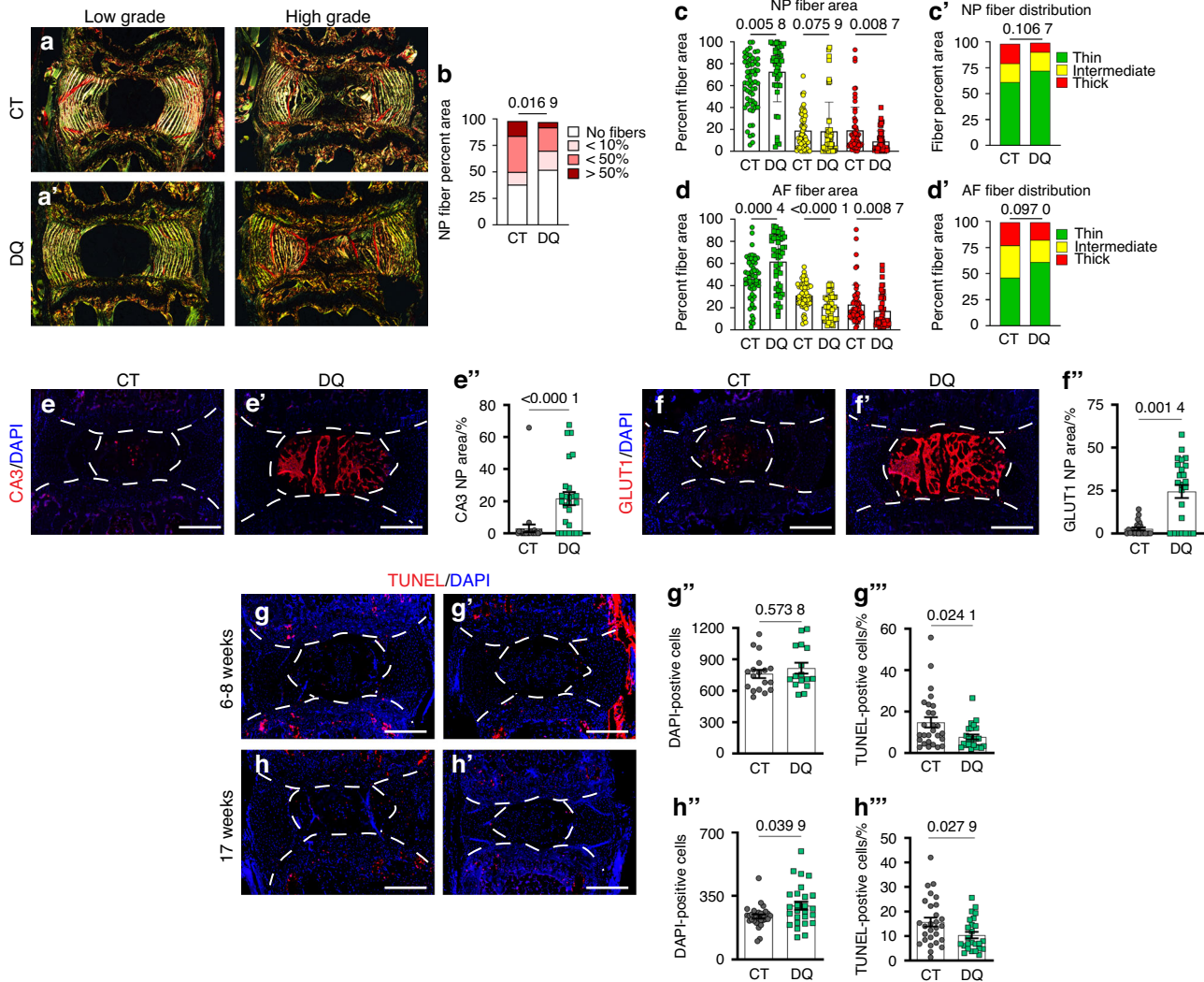


Fig. 3 DQ-treated discs show reduced NP fibrosis, NP cell phenotype retention, and improved cell survival. **a–a'** Quantitative picrosirius red staining indicates that **(b)** DQ-treated discs evidence less NP fibrosis, **(c–c')** with higher proportion of thin (green) collagen fibers in DQ-treated NP tissues, and **(d–d')** AF collagen fiber thickness being significantly altered by DQ treatment. Significantly improved retention of NP phenotypic markers **(e–e')** CA3 and **(f–f')** GLUT1 is observed in DQ mice. **g–g'** At 6–8 weeks, there are not changes in cellularity in DQ mice, but there is a reduction in TUNEL-positive cells. **h–h'** By 17 weeks, TUNEL staining shows **(h')** improved cellularity and **(h'')** a reduction in apoptosis in the discs of DQ-treated mice. Data are shown as mean \pm SD. Significance was determined using an unpaired *t*-test or Mann-Whitney test, as appropriate. Distribution statistics were determined using a χ^2 test. $n_{DQ} = 5-7$, $n_{CT} = 5-7$, 3–4 levels each animal

(Fig. S5J), area (B. Ar.) (Fig. S5K), perimeter (B. Pm.) (Fig. S5L), or cross-sectional thickness (Cs. Th) (Fig. S5M). Together, these results show that DQ treatment minimally affects the vertebral bone, suggesting its safe systemic use for other musculoskeletal tissues.

DQ treatment attenuates degeneration by limiting NP tissue fibrosis

ECM is essential for proper disc function. In SM/J mice, degeneration culminates in the fibrotic remodeling of the matrix, marked by a decrease in proteoglycans and increased collagen deposition,^{20,47} resulting in NP fibrosis, and consequent loss of mechanical properties.^{9,19} Major structural proteins in the disc were evaluated specifically to study fibrotic remodeling in DQ-treated discs. Aligning well with the Modified Thompson Scores of DQ-treated discs, analysis of picrosirius red staining (Fig. 3a–a') showed approximately 25% fewer discs in the DQ cohort had collagen fibers in the NP compartment (Fig. 3b); healthy discs do not have appreciable collagen deposition in the NP. When the fibrotic NP tissues were analyzed, there were no quantitative differences in the collagen fiber thickness in tissues from the DQ

and CT cohorts (Fig. 3c–c'). Analysis of collagen fiber thickness in the AF showed that DQ mice had thinner collagen fibers than CT (Fig. 3d–d'), suggesting DQ delays the fibrotic degenerative phenotype of SM/J mice by increasing collagen remodeling. Interestingly, the abundance of Collagen I (COLI) (Fig. S6A, B'), the aggrecan core protein (ACAN) (Fig. S6C–D'), and chondroitin sulfate (CS) staining (Fig. S4E–F') were similar between the vehicle and DQ treated cohorts, suggesting that the structural collapse of the disc during degeneration precedes increased degradation of these matrix proteins at 17 weeks. On the other hand, DQ treatment led to the reduction of collagen 10 (COL10) (Fig. S6G–G'), often associated with the acquisition of a hypertrophic chondrocyte-like phenotype by NP cells suggesting that DQ facilitates the retention of the NP cell phenotype.

DQ treatment preserves NP cell phenotype

Since NP cells in SM/J mice are known to progressively differentiate into chondrocyte-like cells, we investigated DQ's effects on NP cell phenotype and viability.⁴⁸ Carbonic anhydrase 3 (CA3) and glucose transporter 1 (GLUT1) are known NP

phenotypic markers whose abundance decreases during disc degeneration and aging.^{19,37} Accordingly, NP cells from DQ-treated mice robustly expressed CA3 (Fig. 3e–e′) and GLUT1 (Fig. 3f–f′), and the CT group showed a decreased abundance of these markers. Similarly, discs of DQ-treated mice showed higher NP cellularity and lower percentages of TUNEL-positive cells as early as 6–8 weeks of age (Fig. 3g–g′), resulting in retention of a higher number of cells and consistently lower TUNEL-positive cells at 17-weeks (Fig. 3h–h′). This suggests that DQ treatment mitigates senescence in the disc by preserving the NP cell phenotype and improving cell viability.

DQ treatment results in a distinct transcriptomic signature in the AF and NP compartments

To better understand the possible mechanisms underlying the observed phenotypic improvements in SM/J mice receiving DQ, we performed a global transcriptomic analysis of the NP and AF tissues from 17-week-old CT and DQ cohorts (Fig. 4a). We assessed the baseline differences between treatment groups by analyzing the differentially expressed genes (DEGs, defined by $P \leq 0.05$) in NP (Fig. 4b, c) and AF (Fig. 5a, b) tissues. Hierarchical clustering analysis demonstrated distinct transcriptomic profiles for CT and DQ groups in both tissues (Fig. 4b, Fig. 5a). We identified 382 upregulated DEGs and 441 downregulated DEGs in the NP; 311 upregulated DEGs, and 242 downregulated DEGs in the AF; and 12 commonly upregulated and 21 commonly downregulated DEGs between compartments (Fig. S7A). Commonly upregulated DEGs included *Sel1l2*, *Lonp1*, *Tmem160*, *Raly*, and *Mgat2*; and common downregulated DEGs included *Atf3*, *ler2*, *Zfp36l1*, *Junb*, and *Plaur* (Fig. S7B).

To better understand the biological impact of the DEGs, the CompBio tool (<https://gtac-compbio-ex.wustl.edu>) was used to conduct pathway-level analysis (Fig. 4d, e′, Fig. S7C–D′, Supplementary File 2). In the NP tissues of DQ-treated mice, several related themes forming thematic clusters relating to DNA repair (red cluster) and cell cycle regulation (orange cluster) were identified (Fig. S7C), along with notable themes including *CLRC Ubiquitin Ligase Complex*, *Negative Regulation of Subtelomeric Heterochromatin Assembly*, and *Oxygen-Dependent Proline Hydroxylation of HIF- α* (Fig. S7D–D′). Among the downregulated genes, there was also a significant signature relating to cell cycle regulation (orange cluster), which appeared to coalesce around themes relating to CDKN1A and JNK/TAK signaling (Fig. 4d), along with significantly enriched themes for *TAK-mediated JNK Phosphorylation/Activation* and *p21 Prevents Phosphorylation by Cdh1 by CyclinA:Cdk2* (Fig. 4e–e′). Additionally, there were several themes relating to RNA (purple cluster) and protein (green cluster) regulation (Fig. 4d). Notably, both up- and downregulated DEGs showed themes relating to proline hydroxylation of HIF, and among the downregulated DEGs, there were themes relating to the circadian clock and the cleavage of heparan sulfate from its core proteoglycan.

In the AF, hierarchical clustering also revealed distinct clustering between control and DQ-treated groups (Fig. 5a, b). AF upregulated DEG analysis presented several themes related to development (turquoise cluster), cell cycle (orange cycle), and immune modulation (pink cluster) (Fig. S8A). Notable themes within these clusters included *Hedgehog Signaling Events Mediated by Gli Proteins* and *Internalization of MHC II: li Clathrin Coated Vesicle* (Fig. S8B–B′). Among the downregulated themes, there was again a substantial cell cycle signature (orange cluster), and interestingly, there was a cluster of themes specifically related to JNK/TAK signaling and cell death (Fig. 5c). This is highlighted in themes of *Transcription of E2F Targets Under Negative Control of p107 and p130 in Complex with HDAC1; TAK1 Activates NF- κ B by Phosphorylation/Activation of OKK Complex*; and *TTP, ZFP36 Binds and Destabilizes mRNA* and supports the previous observations that suggest DQ improves degenerative outcomes through the negative regulation of cell cycle arrest and apoptosis (Fig. 5d–d′).

Beyond understanding the impact of DQ in SM/J discs, the molecular mechanisms by which DQ ameliorates the degeneration process in the intervertebral disc are limited. To gain further mechanistic insights, we compared the transcriptomic data from DQ-treated SM/J mice to previously reported findings from DQ-treated aged B6N mice. Direct comparison of the DEGs in the NP from these two mouse models identified 12 upregulated and 33 downregulated common DEGs (Fig. 6a). In the AF, 15 upregulated and 19 downregulated DEGs were common to DQ treatment in SM/J and B6N mice (Fig. 6b). When the downregulated DEGs were compared across both mouse models and disc tissues (NP and AF), we found that only two transcripts were commonly downregulated: *Junb* and *Zfp36l1*, important regulators of senescence fate (Fig. 6c). Moreover, these cross models and disc tissues' common transcripts fortify previous NP and AF gene signature analysis, suggesting JUN signaling as a critical convergence point conferring the benefits of the systemic DQ treatment on disc health.

Though the common downregulation of *Junb* and *Zfp36l1* is a substantial lead into how DQ may mediate disc degeneration, two genes/pathways are insufficient to fully capture the processes driving improved disc health outcomes. Accordingly, we then analyzed the concepts generated in CompBio from DQ vs. CT DEG comparisons to understand the biological processes common to the two treatment models at the pathway level. Assertion engine analysis identified three comparisons to be the most similar at the concept level: upregulated by DQ in SM/J NP and B6N NP; downregulated by DQ in SM/J NP and B6N NP; and downregulated by DQ in SM/J AF and B6N NP (Fig. 6d). Themes that emerged from the SM/J and B6N NP upregulated comparison related to DNA damage, glycosylation, cell cycle, and metabolism; and the SM/J and B6N NP downregulated comparisons had signatures for Jun signaling, metabolism, DNA damage, inflammation, apoptosis, and transcription (Fig. S9A). The comparison between SM/J AF and B6N NP downregulated concepts overlapped with many of these, including inflammation, cell cycle, Jun signaling, and apoptosis (Fig. S9B, C). Notably, these results suggest that in the context of both aging and genetic predisposition models of disc degeneration, DQ improves health outcomes by reducing cell death, and suppressing the activation of inflammatory pathways and that *Junb* may be central to this process.

JUN pathway inhibition mimics the DQ effects in decreasing senescence and SASP in human degenerated NP cells

To better understand the possible link between DQ treatment and JUN downregulation suggested by our bioinformatic studies, we performed an in vitro inhibition study using degenerated human NP cells.⁴³ Accordingly, we compared the effect of DQ treatment with T5224 (a known JUN inhibitor)^{30,49} in the context of an inflammatory stimulus involving SASP molecules, specifically IL-6 and IL-1 β . While we only observed a significant increase in β -Galactosidase (β -Gal) staining in Grade IV cells after inflammatory stimuli, Grades IV and V presented a lower percentage of positive β -Gal-stained cells after DQ treatment (Fig. 7a). Notably, T5224 inhibitor treatments showed a similar effect on Grade IV human cells (Fig. 7a). Furthermore, we measured the expression levels of senescence and SASP markers by qRT-PCR (Fig. 7b, c, Fig. S10A, B). In Grade IV cells, both treatments showed a similar decrease in expression of *CDKN1A* and *IL6* in comparison to the stimulus group. In the Grade V cells, the DQ and JUN inhibitor reduced the expression of *IL6* and *CCL2*. In addition, DQ showed a decrease in *MMP9*, *MMP13* and *VEGF*, while T5224 ameliorated *CDKN1A* and *MMP13* expression. Overall, these studies agreed with bioinformatic findings, suggesting close crosstalk between DQ treatment and JUN inhibition in reducing the senescence burden in human senescent cells.

DISCUSSION

Despite the high global incidence and associated costs of intervertebral disc degeneration and chronic back and neck pain,

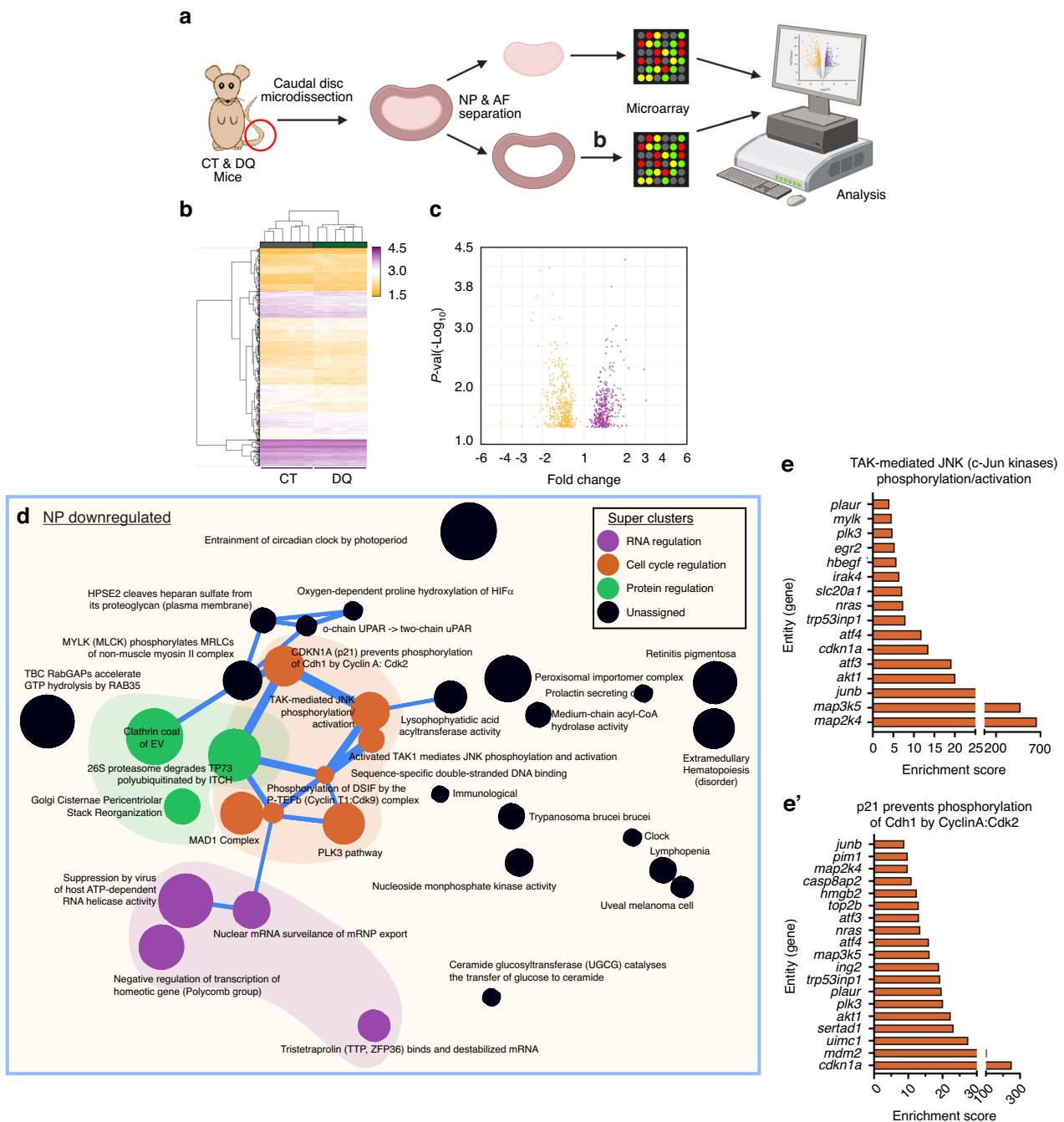


Fig. 4 Transcriptomic analysis of NP tissues highlights possible mechanisms by which DQ improves SM/J disc degeneration. **a** Schematic showing the microarray workflow for analyzing DQ-treated NP and AF tissues. **b, c** Hierarchical clustering of microarray data and volcano plots of 859 DEGs identified in the NP demonstrate distinct clustering of CT and DQ cohorts in NP tissues. **d–e'** Themes relating to the cell cycle (orange), RNA regulation (purple), and protein regulation (green) among the downregulated DEGs in the NP. 4-week-old ($n = 6$), 17-week-old CT and DQ mice ($n = 6$ mice/treatment)

clinical interventions remain primarily limited to symptomatic relief and non-disease modulation.³⁹ This clinical reality is, in part, a result of the complexities underlying disc degeneration and its multifactorial etiology. Among the processes contributing to disc degeneration, cellular senescence is prevalent in degenerative tissues, and its mitigation has shown promise in delaying disc degeneration and back pain.^{10,28,12} Due to its positive correlation with age, senescence is often studied within the context of aging or, in progeria models, posing practical challenges to understanding its contribution to a wide gamut of disc pathologies.^{11,27,50} The recently described SM/J mouse, a model of early-

onset, spontaneous disc degeneration, offers an avenue to study disease phenotypes without using strategies of genetic manipulations or injury to expedite the disease process.^{9,21} Notably, SM/J mice have a comparable lifespan to other inbred strains, such as C57BL/6 and LG/J.¹⁹ Herein, we demonstrate a high senescence burden characterized by p19 and p21 abundance in SM/J discs as early as 4 weeks of age, and the NP and AF transcriptomic profiles during the 17-week degeneration process capture features in the established *SenMayo* gene set, suggesting that cell senescence is part of their degenerative process.⁴⁰ This follows previous work suggesting that senescence in the disc is not solely linked to aging

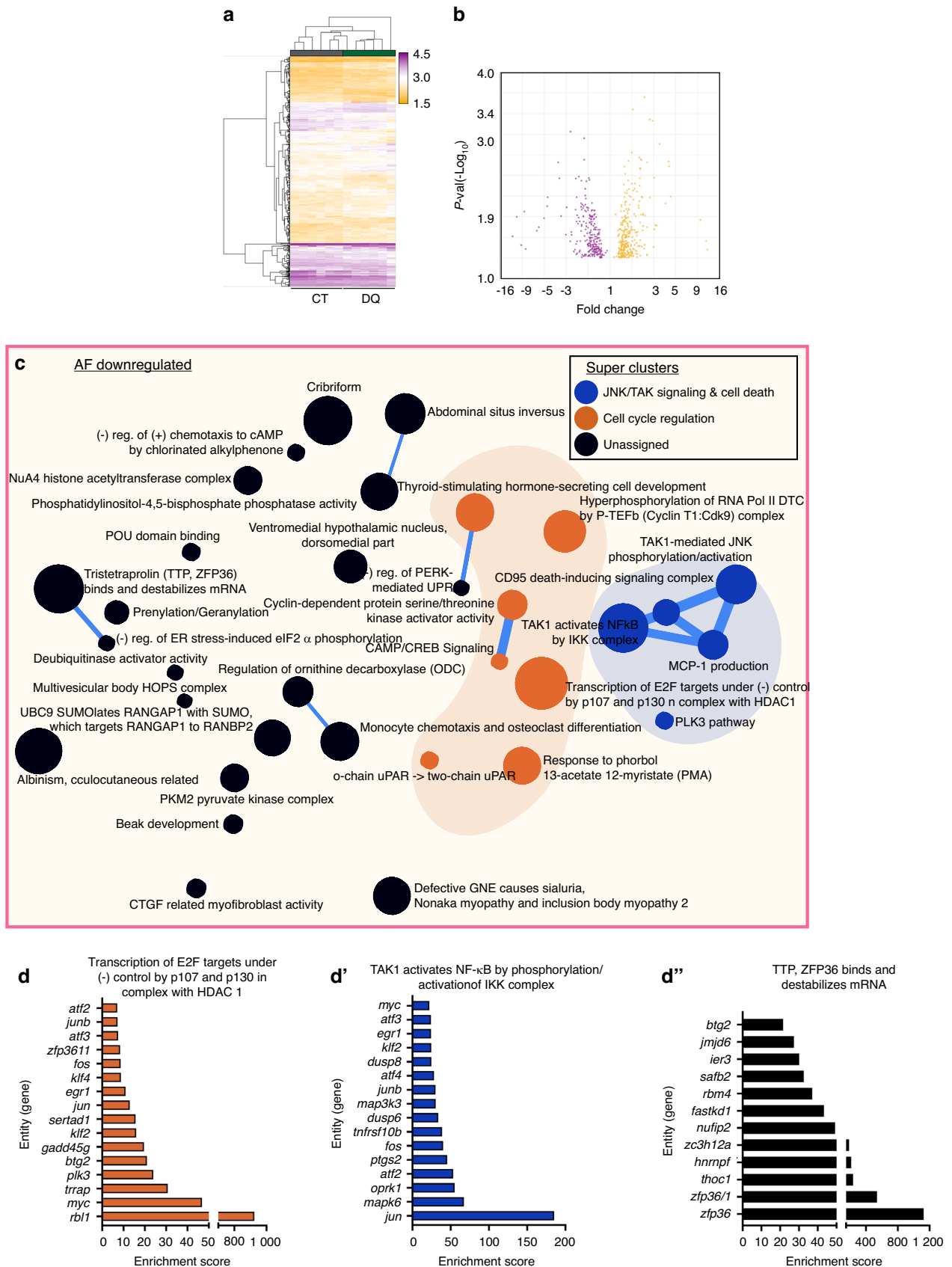


Fig. 5 Transcriptomic analysis of AF tissues highlights possible mechanisms by which DQ improves SM/J disc degeneration. **a** Hierarchical clustering of microarray data demonstrates distinct clustering of CT and DQ cohorts in AF tissues. **b** Volcano plot showing 323 upregulated and 263 downregulated DEGs in the AF of DQ-treated mice. **c–d''** Themes relating to the cell cycle (orange) and JNK/TAK signaling/cell death (blue) among the downregulated DEGs. 17-week-old CT and DQ mice ($n = 6$ mice/treatment)

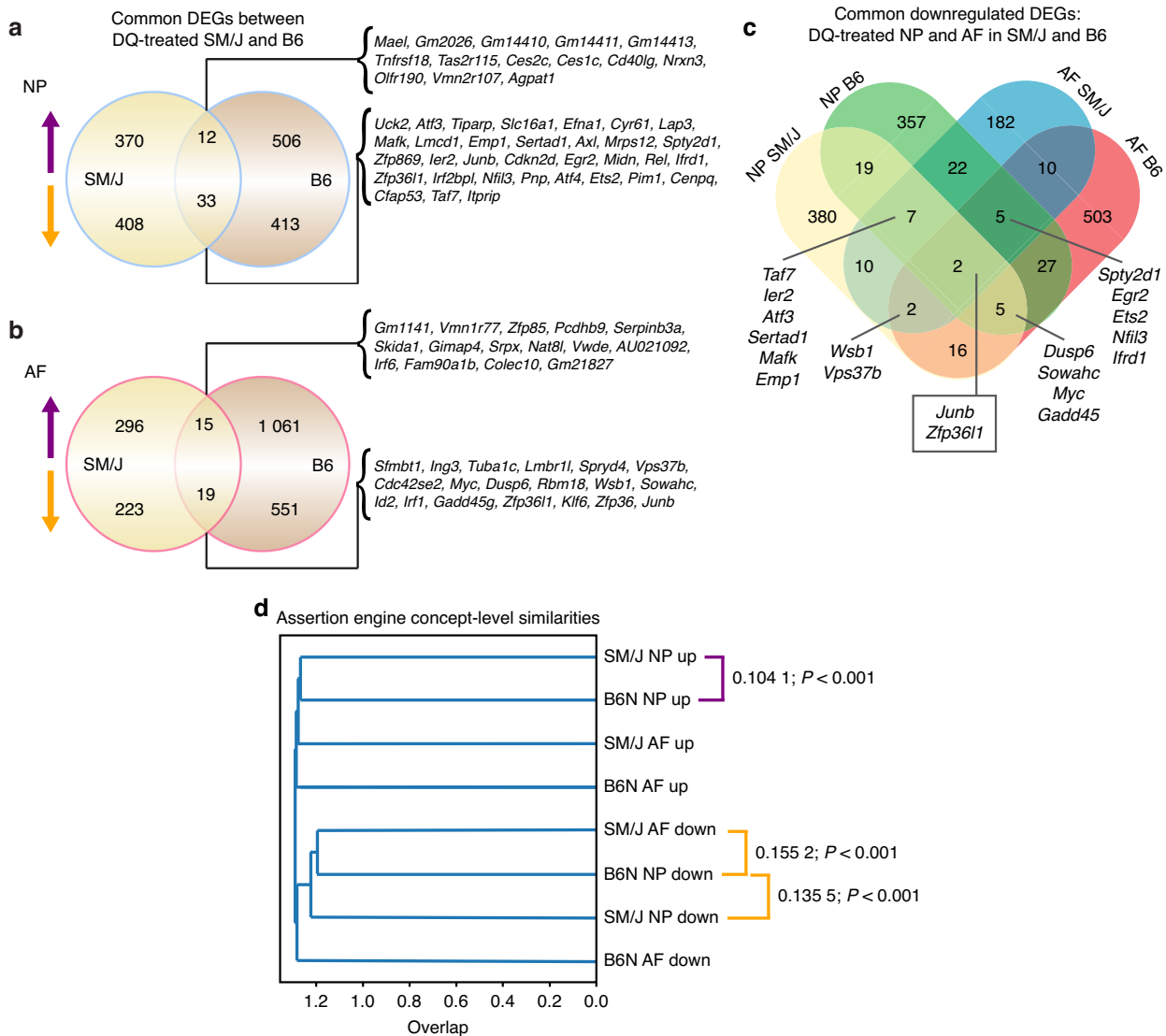


Fig. 6 Comparative analysis of transcriptomic data from DQ-treated SM/J mice and aged B6N mice reveal pathways commonly regulated by DQ. **a** Comparison of DEGs in the NP of DQ-treated SM/J and B6N mice shows 12 commonly upregulated DEGs and 33 commonly downregulated DEGs. **b** Comparison of DEGs in the AF of DQ-treated SM/J and B6N mice shows 15 commonly upregulated DEGs and 19 commonly downregulated DEGs. **c** Analysis of downregulated DEGs in NP and AF tissues from SM/J and B6N mice reveals *Junb* and *Zfp361l* are the only two commonly downregulated DEGs (**d**) Assertion engine analysis identifies three comparisons to be the most similar at the concept level across treatment cohorts and tissues: upregulated by DQ in SM/J NP and B6N NP; downregulated by DQ in SM/J NP and B6N NP; and downregulated by DQ in SM/J AF and B6N NP

but more broadly to degeneration.¹¹ After establishing a correlation between tissue-level senescence and disc degeneration, we investigated the potential of two senotherapeutics – Navitoclax (Nav.) and a Dasatinib and Quercetin (DQ) combination – to ameliorate disc degeneration in SM/J mice, which showed promising outcomes for the DQ cocktail. While we did not evaluate pain behaviors in this study, since discogenic pain is evident in SM/J mice after 18 months following the onset of herniations,²⁰ promising results from Manarion et al. have shown a strong effect of senolytic strategies in preventing back pain.²⁸ Here, we focused on understanding the role of senescence in promoting early disc degeneration in SM/J intervertebral disc. Thus, by cross-referencing the transcriptomic signature of DQ SM/J mice with our previous work on aging B6N mice¹⁹ and further exploring the mechanistic response of human NP cells in vitro to DQ treatment and JUN inhibition, we found that DQ reduces degenerative outcomes by limiting cell death, decreasing the senescence burden, and SASP and downregulation of the JUN

pathway may play a key role in the process (Figs. 6, 7). Additionally, this work establishes SM/J mice as a model for studying the contribution of senescence to disc degeneration and supports the utility of DQ as a senotherapeutic agent that works by preventing disease progression, rather than selectively killing senescent cells to promote tissue repopulation.

In human intervertebral discs, a positive correlation between degeneration and local senescence is established.¹¹ Additionally, in aging mice, systemic elimination of cells positive for p16^{INK4a}, an important marker of cell senescence,⁵¹ demonstrates a clear causality between disc degeneration and senescence.²⁷ In recent years, senotherapeutics have been shown to selectively target senescent cells in a variety of cell and tissue types by interfering with their unique pro-survival pathways, such as JAK1/2, BCL-2/BCL-XL, PI3K/AKT, p53/p21/Serpines, dependence receptors/tyrosine kinases, and the HIF-1 α pro-survival mechanism.⁵² Among these therapeutics, Navitoclax (ABT263) has shown promise in chondrocytes, cartilage tissue culture, and hip explant cultures,

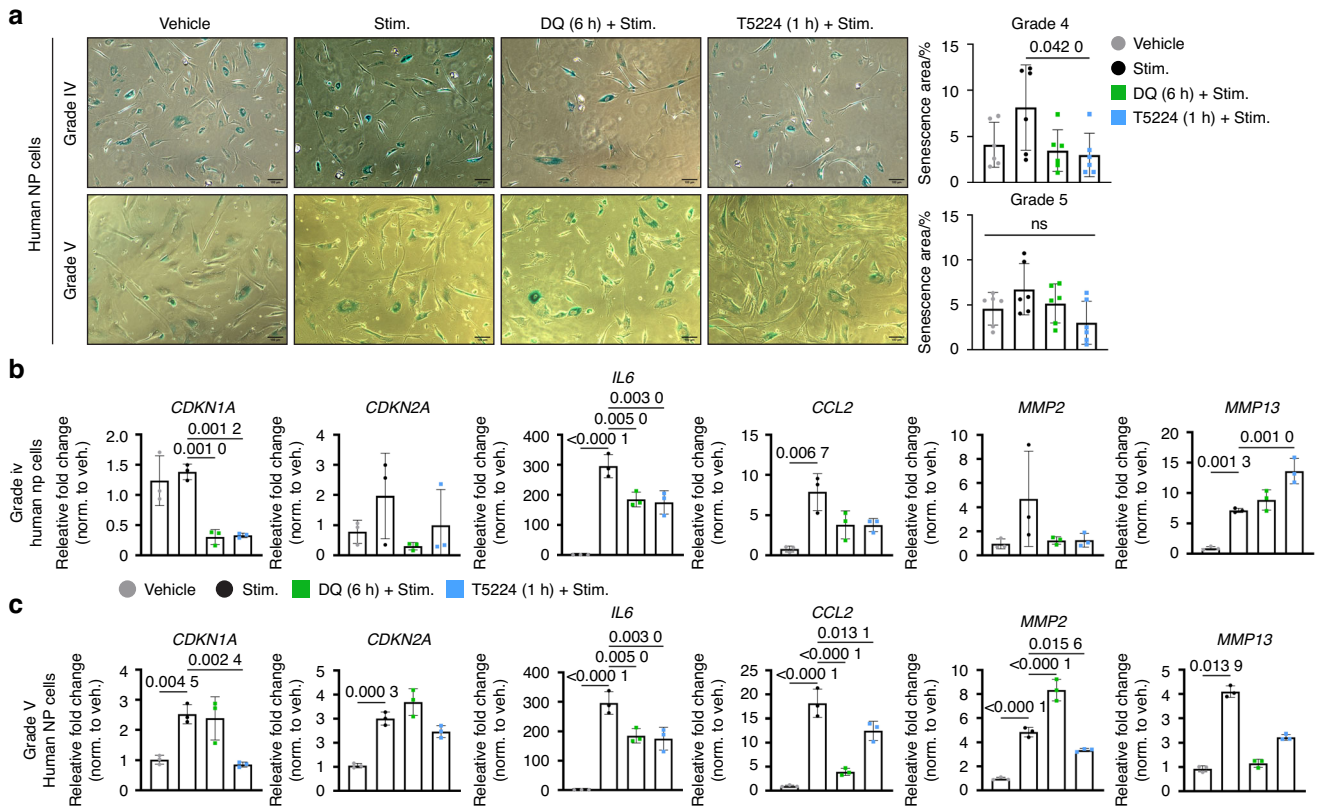


Fig. 7 JUN pathway inhibition mimics the positive effect of DQ in decreasing senescence and SASP in human degenerated NP cells. **a** Grade IV and V human degenerated NP cells show a lower percentage of β -Gal-staining after treatment with DQ and JUN inhibitor, or only DQ, respectively. **b** Grade IV Human NP cells exhibit lower expression of *IL-6*, *MMP2*, and *MMP13* compared to the stimulus group. Additionally, DQ treatment resulted in a decrease in *CDKN1A* and *IL-6*, while T5224 enhanced *MMP13* expression. **c** Grade V human NP cells exhibit lower expression of *CDKN1A*, *CDKN2A*, *IL-6*, *CCL2*, *MMP2*, and *MMP13* relative to the stimulus group. DQ treatment attenuated the expression of *IL-6* and *MMP2*. T5224 ameliorated *CDKN1A*, *IL-6*, *CCL2*, and *MMP2* expression. Data are shown as mean \pm SD. Significance was determined using Dunnett's multiple comparisons test ($n = 3$ independent experiments, performed in triplicate)

with results demonstrating the ability of the drug to selectively clear senescent cells and reduce SASP.⁵³ Similarly, in an injury-induced model of disc degeneration, local injection of Nav. to the injured disc improved structural degeneration and reduced the local senescence and SASP.⁵⁴ By contrast, our results demonstrate that systemic Nav. administration is insufficient to alleviate the disc tissue senescence burden in SM/J, possibly explaining the failure to affect degenerative outcomes and supporting the causal link between disc senescence and degeneration progression. This finding suggests that the efficacy of Nav. in the disc is limited to the context of local administration or possibly dependent on the local concentration of the drug. Intradiscal injection, however, poses the risk of propagating damage to the disc by introducing a new acute injury, as suggested by animal studies and a landmark study on discography in human patients by Carragee and colleagues, necessitating further investigation of potential mitigators of disc degeneration that can be systemically delivered.⁵⁵ Additionally, our results suggest that, in the context of disc senescence, simultaneous inhibition of ephrin B (using Dasatinib) and the PI3K/AKT pathways (using Quercetin) is more effective than targeting BCL-XL/BCL-W and MCL-1 with Nav.⁵⁶ These findings align with recent reports by Sanborn et al., which highlight the tissue-specific nature of senescence signatures and further emphasize that the efficacy of senotherapeutic strategies is highly context-dependent, varying according to tissue type, therapeutic window, and dosage.^{12,28,47}

One of the major consequences of tissue degeneration in a vast majority of age-related diseases, such as dementia, glaucoma, chronic obstructive disease, and musculoskeletal pathologies, is

local fibrosis and loss of matrix homeostasis.⁴⁴ The intervertebral disc is no exception, with fibrosis being one of the major disc degeneration subphenotypes characterized by reduced shock absorption, spine flexibility, and disc height, culminating in back pain.^{9,20} We have previously shown that p16, a master regulator of senescence, modulates SASP and matrix composition during aging in the intervertebral disc.⁵⁰ Similar to the aging B6N model, DQ treatment in the present study promoted lower rates of NP fibrosis, evidenced by lower TGF- β levels.⁴⁵ Moreover, DQ promoted the retention of the NP cell phenotype, with a lower acquisition of a hypertrophic chondrocyte-like phenotype, as demonstrated by the reduced abundance of COLX.⁹ While DQ treatment did not achieve total mitigation of disc degeneration, it may have improved the local plasticity of cells to respond to stressors, delaying degeneration and promoting local extracellular matrix function. In this context, modulation of Arp2/3 signaling and actin cytoskeleton by DQ treatment supports this rationale by implying cellular osmoadaptation to the local environment.⁴⁶

Systemic DQ treatment has been shown to effectively target senescent cells⁹ in human disease contexts, with a growing number of clinical studies investigating its efficacy for disorders ranging from fibrotic NAFLD to skeletal health during aging.^{34,35} Previously, DQ showed positive effects in the context of age-associated disc degeneration.⁴² In the current study, we tested the DQ regimen in the SM/J mice, a model of early-onset disc degeneration, one of the main causes of back pain in middle-aged adults.⁴⁸ As was previously observed in B6N mice treated with DQ, complete rescue of the degenerative phenotype was not observed

in SM/J mice; however, significant improvements to tissue and cellular morphology were observed at 6–8 weeks and 17 weeks. Improved morphological outcomes were accompanied by a reduction in senescence markers and SASP in NP and AF tissues, indicating that systemic DQ treatment can successfully modulate cell behavior in the disc microenvironment. Of particular interest are our findings on reduced cell death and better retention of NP cell phenotypic markers in the discs of DQ-treated SM/J mice. This was also observed in the DQ aging B6N mice model, where DQ treatment improved degenerative outcomes by limiting cell senescence, which prevents SASP, cell death, and consequent degeneration.⁴² Senescent cells are typically considered to have entered a state of permanent cell cycle arrest, and the central dogma of senolytic drugs is that they selectively kill senescent cells, enabling non-senescent cells to repopulate the tissue with healthier cells and better maintain tissue homeostasis.⁵² Our results, however, suggest that DQ impacts the disc in an alternative or complementary fashion, promoting cell survival and retention of the native cell phenotype, which limits cell death and degeneration of the disc. The cells in the disc are post-mitotic, so if senolytic drugs led to the death of senescent cells, it is unlikely the remaining cells would repopulate the compartment, which is shown by a lower rate of cell loss between 6–8 and 17 weeks in DQ-treated SM/J mice. Additionally, initiating cell death in a sparsely populated compartment could potentially further propagate damage to the tissue.⁵⁷ Supporting this idea, there is evidence that cell senescence could be reversible through p16/p53 axis^{58,59} providing some basis for the hypothesis that DQ senotherapeutics enabled the survival of the existing cells and preserved their phenotype. Our findings are mimicked by senostatics, which, for example, in osteoarthritis, can modulate STING and NF- κ B pathways, preventing apoptosis and senescent cell fate.^{60,61} While in the context of the disc, the cGAS-STING pathway alone does not prevent senescence progression,⁶² prolonged activation of NF- κ B has been shown to accelerate disc degeneration through increased local production of inflammatory cytokines, chemotactic proteins, and catabolic enzymes.⁶³ Thus, we hypothesize that DQ inhibition of JUN signaling, and consequently JUN-NF- κ B cross-talk, may play a crucial role in promoting disc cell survival and maintaining disc tissue homeostasis.⁶⁴ These findings support the idea that the success of a senotherapeutic regimen is dependent on tissue type, pathology, administration route/ time, and the signaling pathways it may target.^{35,42}

Notably, when overlapping the *universal organismal aging genes* in mice, comprising 76 cell-type-specific signatures from Tabula Muris Senis, with established senescence marker panels, Jun emerged as one of the only three common upregulated genes.⁴⁷ Consistently, both DQ-treated SM/J mice and aged B6N models showed downregulation of JNK pathway activation, known to regulate senescence and *Cdkn2a* (*p16*) expression, accompanied by reduced senescence markers across intervertebral disc compartments.⁶⁵ Similarly, a shared downregulation across NP and AF tissues of *Junb* and *Zfp3611* was noted in these models. It is important to note that JUNB has been shown to regulate the feedforward network of TGF β signaling promoting sustained activation of genes involved in cell adhesion, ECM function, and epithelial-mesenchymal transition.⁶⁶ Similarly, JUN forms a positive regulatory circuit with an important SASP factor IL6, thereby promoting a profibrotic response.⁶⁷ These findings suggest that the downregulation of *Junb* by DQ treatment not only attenuates senescence-associated features, including cell cycle arrest and SASP markers, but may also directly contribute to reduced fibrosis, decreasing the expression of critical local and systemic mediators, such as IL-6 and TGF- β . This positions JUNB as a potential therapeutic target for alleviating disc senescence and intervening in disc fibrosis (Fig. S10C). Interestingly, the inhibition experiments provided strong evidence linking the DQ

effect on human degenerated NP cells to the JUN pathway. T5225 is currently in a stage II clinical trial for rheumatoid arthritis,³⁰ and there is growing evidence about its senotherapeutic potential to reduce local SASP burden.⁴⁹ Despite the positive results of both in vitro and preclinical studies, the path to bringing the senotherapeutic strategy to the clinic is still hindered by the need to identify who would benefit from these treatments, when they should be administered, and for how long they should be continued.

Regarding disc cell homeostasis, in both models, at a thematic level, DQ treatment resulted in downregulating various genes related to DNA damage, inflammation, and apoptosis. Reductions in DNA damage and inflammatory signatures may be indicative of lower senescence and SASP burdens in the tissues, and a reduced apoptotic signature further supports DQ treatment, prolonging the survival of cells. Notably, in SM/J mice, AF tissues from DQ-treated mice showed enrichment for hedgehog signaling, which is critical for maintaining disc health and could indicate one means by which DQ treatment preserves disc cell phenotypes.^{68,69}

In summary, our findings in a model of early-onset disc degeneration build on previous findings in aging B6N mice and provide further evidence for the beneficial effects of systemic administration of DQ, but not Navitoclax to improve health outcomes in the disc.^{9,42} We also show that SM/J mice are a model of senescence-associated disc degeneration, providing the field with the benefit of a model of spontaneous disc degeneration and senescence without the constraints of waiting for animals to age or performing complex genetic manipulations. Evidence supports that DQ treatment in both SM/J and aging B6N mice improves degenerative outcomes in the disc by promoting cell survival, limiting the progression of senescence and SASP, and ameliorating intervertebral disc fibrosis. Excitingly, our results suggest a new link between DQ treatment and JUN pathway downregulation, which may underscore the beneficial effects of DQ in NP and AF tissues, paving way for future studies to investigate this mechanism.

MATERIALS AND METHODS

Mice, treatment, and study design

Animal procedures were performed under approved protocols by the IACUC of Thomas Jefferson University. SM/J (Stock #000687, Jackson Labs) and C57BL/6 J (Stock #000664, Jackson Labs) were bred and raised at Thomas Jefferson University. For preliminary histological analyses SM/J ($n=5$) and C57BL/6 J ($n=8$) were collected at 4 weeks of age. Beginning at 4 weeks of age, mice received a weekly intraperitoneal injection of either 40 mg/kg Navitoclax (Nav.), 5 mg/kg Dasatinib with 50 mg/kg Quercetin (DQ), or a PBS and DMSO vehicle control (CT). Animals received this treatment until they were 6–8 weeks old ($n=7$ mice/treatment group, DQ and CT only) or 17 weeks old ($n_{CT}=19$ (9 F, 10 M), $n_{DQ}=17$ (9 F, 8 M); $n_{Nav.}=7$ (3 F, 4 M), $n_{Veh.}=7$ (3 F, 4 M)). These timepoints were selected based on previous studies showing mildly degenerative caudal disc tissue at 4 weeks old, significant cell death at 8 weeks, and severe fibrotic disc degeneration by 17 weeks.^{9,21}

Tissue Processing, μ CT Analysis, and Histology

Caudal spine motion segments Ca5–Ca9 were dissected and immediately fixed in 4% PFA in PBS at 4 °C for 48 hours. Following fixation, μ CT scans (Bruker Skyscan 1275; Bruker, Kontich, Belgium) were performed. An aluminum filter was used, and all scans were conducted at 50 kV and 200 μ A, with an exposure time of 85 ms, yielding a resolution of 15 μ m. Three-dimensional image reconstructions were generated, and all subsequent analyses were conducted using Bruker programs NRecon, CTan, and CTVox.). $n_{CT}=8$ mice (5 F, 3 M), $n_{DQ}=6$ mice (3 F, 3 M); 3–5 vertebrae/mouse, 4 discs/mouse.

Motion segments then underwent 21 days of decalcification in 20% EDTA at 4 °C, followed by paraffin embedding. Coronal sections of 7 µm were generated, and HistoClear deparaffinization followed by graded ethanol rehydration preceded all staining protocols.

Safranin O/Fast Green/Hematoxylin staining was conducted and visualized using 5x/0.15 N-Achroplan and 20x/0,5 EC Plan-Neofluar (Carl Zeiss) objectives on an AxioImager 2 microscope and Zen2™ software (Carl Zeiss Microscopy). This staining was used to evaluate disc structure, and four blinded graders scored NP and AF compartments using Modified Thompson Grading. Picosirius red staining was conducted and imaged in the brightfield and under polarized light using 4x Pol/W/D 7.0 objectives on an Eclipse LV100 POL microscope (Nikon). NIS Elements Viewer software (Nikon) was then used to evaluate the areas of the disc occupied by green (thin fibers), yellow (intermediate fibers), or red (thick pixels) pixels. NP fibrosis was also quantified according to the percentage of the NP space occupied by collagen fibers.

Immunohistology and cell number measurements

For all immunohistochemical stains, antibody-specific antigen retrieval was conducted by way of incubation in either chondroitinase ABC for 30 min at 37 °C, hot citrate solution (pH 6) for 40 min, or proteinase K for 8 min at room temperature. Tissue sections were then blocked in 2%–10% normal serum in PBS-T, and incubated with antibodies against p19 (1:100, Novus NB200-106), p21 (1:200, Novus NB100-1941), collagen I (1:100, Abcam ab34710), aggrecan (1:50; Millipore; AB1031), chondroitin sulfate (1:300, Abcam ab11570), IL-1b (1:100, Novus NB600-633), IL-6 (1:50, Novus NB600-1131), TGFb (1:100; Abcam; ab92486), collagen X (1:500, Abcam ab58632), CA3 (1:150, Santa Cruz), and GLUT-1 (1:200, Abcam, ab40084). For GLUT1, a M.O.M. kit (Vector laboratories, BMK-2202) was used for blocking and primary antibody incubation. Tissue sections were washed with PBS-T and incubated in the dark with the appropriate Alexa Fluor® -594 or -488 conjugated secondary antibody (1:700; Jackson ImmunoResearch Laboratories, Inc.) for one at room temperature. TUNEL staining was conducted using an in situ cell death detection kit (Roche Diagnostic; 12156792910) according to manufacturer's specifications. All stained sections were washed with PBS-T and mounted with ProLong™ Diamond Antifade Mountant with DAPI (Fisher Scientific, P36971). Stains were visualized with an AxioImager 2 (Carl Zeiss Microscopy), using 5x/0.15 N-Achroplan and 20x/0,5 EC Plan-Neofluar objectives, an X-Cite® 120Q Excitation Light Source (Excelitas Technologies), AxioCam MRm camera (Carl Zeiss Microscopy), and Zen2™ software (Carl Zeiss Microscopy). Exposure settings remained constant across treatments for each stain.

Digital image analysis

All immunohistochemical quantification was conducted in grey-scale using the Fiji package of ImageJ.⁷⁰ Images with a selected ROI (NP and AF EP) were thresholded to subtract the background, transformed into binary format, and then staining area and cell number were calculated using the *analyze particle* function in Image J software, v1.53e.^{9,34}

Circulating Cytokine Analysis

Blood was collected by intracardiac puncture following sacrifice and centrifuged at 1 500 r/min, at 4 °C for 15 min to isolate the plasma, which was stored at -80 °C until analysis. Levels of proinflammatory proteins and cytokines were analyzed using V-PLEX Mouse Cytokine 19-Plex Kit (Meso Scale Diagnostics, K15255D) according to manufacturer's specifications.

Tissue RNA Isolation and Microarray Analysis

NP and AF tissues were dissected from caudal discs (Ca1-Ca15) of 4-week-old ($n=6$), 17-week-old CT and DQ mice ($n=6$ mice/treatment). Pooled tissue from a single animal served as an

individual sample. Samples were homogenized, and total RNA was extracted using the RNeasy® Mini kit (Qiagen). The purified, DNA-free RNA was converted to cDNA using the EcoDry™ Premix (Clontech). Template cDNA and gene-specific primers (IDT, IN) were added to Power SYBR Green master mix, and expression was quantified using the Step One Plus Real-time PCR System (Applied Biosystems).

Total RNA with RIN > 4 was used for the analysis. Fragmented biotin-labeled cDNA was synthesized using the GeneChip WT Plus kit according to the ABI protocol (Thermo Fisher). Gene chips (Mouse Clariom S) were hybridized with biotin-labeled cDNA. Arrays were washed and stained with GeneChip hybridization wash & stain kit and scanned on an Affymetrix Gene Chip Scanner 3000 7 G, using the Command Console Software. Quality Control of the experiment was performed in the Expression Console Software v 1.4.1. CHP files were generated by sst-rma normalization from Affymetrix.CEL files, using the Expression Console Software. Only protein-coding genes were included in the analyses. Detection above background higher than 50% was used for Significance Analysis of Microarrays (SAM), and the p-value was set at 5%. Gene-level analyses and visualizations were conducted in the Affymetrix Transcriptome Analysis Console (TAC) 4.0 software. To explore the biological significance of the DEGs, these were cleaned using Panther HITS protein⁷¹ and duplicates were removed. FDR and log fold settings were used for the gene lists as follows: 4–17 weeks, AF: FC ≥ 2, FDR < 0.001; NP: FC > 2, FDR < 0.05; SM/J DQ vs. Veh. 17-weeks; AF and NP: p-value < 0.05. Array data are deposited in the GEO database, GSE281300.

Bioinformatic Analysis

Significantly differentially up- and downregulated genes from the NP and AF compartments were cleaned for only protein-coding genes using PANTHER classification system database⁷¹ and enriched analyzed using the GTAC-CompBio Analysis Tool (<https://gtac-compbio-ex.wustl.edu>, St. Louis, MO).^{5,37} CompBio performs a literature analysis to identify relevant biological processes and pathways represented by the input differentially expressed entities, in this case, DEGs. This is accomplished with an automated Biological Knowledge Generation Engine (BKGE) that extracts all abstracts from PubMed that reference entities of interest (or their synonyms), using contextual language processing and a biological language dictionary that is not restricted to fixed pathway and ontology knowledge bases. Conditional probability analysis is utilized to compute the statistical enrichment of biological concepts (processes/pathways) over those that occur by random sampling. Related concepts built from the list of differentially expressed entities are further clustered into higher-level themes (e.g., biological pathways/ processes, cell types, and structures, etc.). Within CompBio, scoring of entity (DEG), concept, and overall theme enrichment is accomplished using a multi-component function referred to as the Normalized Enrichment Score (NES). The first component utilizes an empirical p-value derived from several thousand random entity lists of comparable size to the user's input entity list to define the rarity of a given entity-concept event. The second component, effectively representing the fold enrichment, is based on the ratio of the concept enrichment score to the mean of that concept's enrichment score across the set of randomized entity data. As such, the NES reflects the rarity of the concept event associated with an entity list, as well as its degree of overall enrichment. Complete thematic, entity, and concept-level data for analyses conducted in control and DQ-treated NP and AF tissues are included in Supplementary File 2.

The program was further used to compare the NP and AF profiles from DQ-treated SM/J mice with deposited NP and AF profiles from DQ-treated aged B6N mice (GSE154619) at the concept level. This was done by identifying the biological terms/concepts common across datasets and running those concepts as entities to acquire common themes across projects. An assertion

engine tool was also used to determine which comparisons across projects were most similar.

Human NP in vitro study design

Human cervical NP cells harvested from grade IV and V Pfirrmann score discs were plated at passage 3–4, in Dulbecco's modified Eagle's medium (DMEM) and 10% fetal bovine serum (FBS) supplemented with antibiotic-antimycotic solution in a humidified atmosphere containing 5% CO₂ at 37°C.⁴³ Cells were then split in 4 groups and plated for 24 h: Vehicle control (DMSO 0.1%); stimulus only IL-1β (10 ng/mL)⁷² and IL-6 (0.8 ng/mL)⁷³ (#200-01B and #200-06; PeproTech), DQ treatment (Dasatinib 0.25 μmol/L + Quercetin 10 μmol/L)^{74,75} plus stimulus; and T-5224 inhibitor (30 μmol/L)^{49,76} (#SML3778, Sigmaalrich) plus stimulus.

Real-time Quantitative RT-PCR

Total RNA from Human Grade IV and V NP cells were extracted, the purity was determined by measuring the absorbance at 260 and 280 nm. The isolated RNA was then converted into cDNA. The cDNA thus obtained was subjected to real-time polymerase chain reaction (qRT-PCR) using gene-specific primers by SYBR Green chemistry, and mRNA expression was measured using the StepOnePlus System. Expression was normalized to *Hprt1*. Melting curve analysis confirmed specificity and absence of primer dimers. Samples were run in triplicates with template-free controls; all primers were from Integrated DNA Technologies.

Senescence-associated β-galactosidase (SA-β-Gal) staining

Cells were grown in collagen coated 12-well plates were washed with PBS, fixed for 10 minutes, and stained with 1 mg/ml X-Gal solution following the manufacturer's instructions (Cell Signaling Technology, #9860). After overnight incubation at 37°C without CO₂, cells were washed and examined under a bright-field microscope 10x (EVOS M5000 Invitrogen). Each sample was run in technical triplicate.

Statistical analyses

All statistical analyses were performed using Prism10 (GraphPad, La Jolla). Data are represented as mean ± SD. Data distribution was assessed with the Shapiro-Wilk normality test, and the differences between the two groups were analyzed by *t*-test or Mann-Whitney, as appropriate. Dunnett's multiple comparisons test for multiple group comparison. A χ² test was used to analyze the differences between the distribution of percentages. *P* ≤ 0.05 was considered a statistically significant difference.

DATA AVAILABILITY

The microarray dataset that supports the findings of this study is openly available in the GEO database, accession number GSE281300.

ACKNOWLEDGEMENTS

We thank Victoria A. Tran, Thomas Jefferson University, for her assistance with the micro-CT analysis.

AUTHOR CONTRIBUTIONS

Conceptualization: E.J.N., O.K.O., M.V.R.; Methodology: E.J.N., O.K.O., S.J., M.V.R.; Investigation: E.J.N., O.K.O., S.J., E.A., R.A.B.; Visualization: E.J.N., O.K.O., R.A.B.; Funding acquisition: M.V.R., E.J.N.; Project administration: M.V.R.; Supervision: M.V.R.; Writing – original draft: O.K.O., E.J.N., M.V.R.; Writing – review & editing.

FUNDING

This study is supported by the grants from the National Institute of Arthritis and Musculoskeletal and Skin Diseases (NIAMS) R01AR055655, R01AR064733, and R01AR074813, and the Michael Michelson Gift Fund to MVR. E.J.N. received a PhD fellowship (PD/BD/128077/2016) from the MD/PhD Program at the University of Minho, funded by the Fundação para a Ciência e a Tecnologia (FCT).

ADDITIONAL INFORMATION

Supplementary information The online version contains supplementary material available at <https://doi.org/10.1038/s41413-026-00526-4>.

Competing interests: The authors declare no competing interests.

REFERENCES

- Collaborators GBD 2017 Disease and Injury Incidence and Prevalence. Global, regional, and national incidence, prevalence, and years lived with disability for 354 Diseases and Injuries for 195 countries and territories, 1990–2017: A systematic analysis for the Global Burden of Disease Study 2017. *Lancet* **392**, P1789–P1858 (2018).
- Teraguchi, M. et al. Prevalence and distribution of intervertebral disc degeneration over the entire spine in a population-based cohort: the Wakayama Spine Study. *Osteoarthritis Cartil.* **22**, 104–110 (2014).
- Shapiro, I. M. & Risbud, M. V. *The Intervertebral Disc: Molecular and Structural Studies of the Disc in Health and Disease*. <https://doi.org/10.1007/978-3-7091-1535-0> (2002).
- Christ, B., Huang, R. & Scaal, M. Formation and differentiation of the avian sclerotome. *Anat. Embryol.* **204**, 333–350 (2004).
- Madhu, V. et al. The mitophagy receptor BNIP3 is critical for the regulation of metabolic homeostasis and mitochondrial function in the nucleus pulposus cells of the intervertebral disc. *Autophagy* **19**, 1821–1843 (2023).
- Silagi, E. S. et al. Lactate Efflux From Intervertebral Disc Cells Is Required for Maintenance of Spine Health. *J. Bone Miner. Res.* **35**, 550–570 (2020).
- Iatridis, J. C., Michalek, A. J., Purmessur, D. & Korecki, C. L. Localized intervertebral disc injury leads to organ level changes in structure, cellularity, and biosynthesis. *Cell Mol. Bioeng.* **2**, 437–447 (2009).
- Ohnishi, T., Novais, E. J. & Risbud, M. V. Alterations in ECM signature underscore multiple sub-phenotypes of intervertebral disc degeneration. *Matrix Biol.* **6–7**, 100036 (2020).
- Choi, H. et al. A novel mouse model of intervertebral disc degeneration shows altered cell fate and matrix homeostasis. *Matrix Biol.* **70**, 102–122 (2018).
- Novais, E. J., Diekmann, B. O., Shapiro, I. M. & Risbud, M. V. p16 Ink4a deletion in cells of the intervertebral disc affects their matrix homeostasis and senescence associated secretory phenotype without altering onset of senescence. *Matrix Biol.* **82**, 54–70 (2019).
- Le Maitre, C. L., Freemont, A. J. & Hoyland, J. A. Accelerated cellular senescence in degenerate intervertebral discs: A possible role in the pathogenesis of intervertebral disc degeneration. *Arthritis Res. Ther.* **9**, R45 (2007).
- Novais, E. J. et al. Long-term treatment with senolytic drugs Dasatinib and Quercetin ameliorates age-dependent intervertebral disc degeneration in mice. *Nat. Commun.* **12**, 5213 (2021).
- Battié, M. C., Videman, T., Levälähti, E., Gill, K. & Kaprio, J. Genetic and environmental effects on disc degeneration by phenotype and spinal level: a multivariate twin study. *Spine (Phila. Pa 1976)* **33**, 2801–2808 (2008).
- Battié, M. C. et al. The Twin Spine Study: Contributions to a changing view of disc degeneration. *Spine J.* **9**, 47–59 (2009).
- Annullun, S. et al. An allele of COL9A2 associated with intervertebral disc disease. *Science*. **285**, 409–412(1999).
- Takahashi, M. et al. The association of degeneration of the intervertebral disc with 5a/6a polymorphism in the promoter of the human matrix metalloproteinase-3 gene. *J. Bone Joint Surg. - Series B* **83**, 491–495 (2001).
- Huang, X. et al. Interleukin 6 (IL-6) and IL-10 promoter region polymorphisms are associated with risk of lumbar disc herniation in a northern Chinese Han population. *Genet. Test Mol. Biomarkers* **21**, 17–23 (2017).
- Toktaş, Z. O. et al. Association of collagen I, IX and vitamin D receptor gene polymorphisms with radiological severity of intervertebral disc degeneration in Southern European Ancestor. *Eur. Spine J.* **24**, 2432–2441(2015).
- Novais, E. J. et al. Comparison of inbred mouse strains shows diverse phenotypic outcomes of intervertebral disc aging. *Aging Cell* **19**, e13148 (2020).
- Novais, E. J. et al. Neuroimmune changes underscore pain-associated behaviors and disc herniations in SM/J mice. *bioRxiv* <https://doi.org/10.1101/2024.02.23.581794> (2024).
- Zhang, Y. et al. Early onset of disc degeneration in SM/J mice is associated with changes in ion transport systems and fibrotic events. *Matrix Biol.* **70**, 123–139 (2018).
- Vo, N. et al. Accelerated Aging of Intervertebral Discs in a Mouse Model of Progeria. *J. Orthop. Res.* **100**, 130–134 (2012).
- REICH, M. S., JARVIS, J. P., SILVA, M. J. & CHEVERUD, J. M. Genetic relationships between obesity and osteoporosis in LGXSM recombinant inbred mice. *Genet Res (Camb.)* **90**, 433–444 (2008).
- Shingo, H., Rai, M. F., Janiszak, K. L., Cheverud, J. M. & Sandell, L. J. Sandell Cartilage and Bone Changes during Development of Post-Traumatic Osteoarthritis in Selected LGXSM Recombinant Inbred Mice. *Osteoarthritis Cartil.* **20**, 562–571 (2012).
- Muñoz-espín, D. & Serrano, M. Cellular senescence: from physiology to pathology. *Nat. Rev. Mol. Cell Biol.* **15**, 482–496 (2014).

26. Zhu, Y. et al. New agents that target senescent cells: The flavone, fisetin, and the BCL-XL inhibitors, A1331852 and A1155463. *Aging* **9**, 955–963 (2017).
27. Patil, P. et al. Systemic clearance of p16INK4a-positive senescent cells mitigates age-associated intervertebral disc degeneration. *Aging Cell* **18**, e12927 (2019).
28. Mannarino, M. et al. Senolytic treatment for low back pain. *Sci. Adv.* **11**, (2025).
29. Cherif, H. et al. Senotherapeutic drugs for human intervertebral disc degeneration and low back pain. *Elife* **9**, e54693 (2020).
30. Ye, N., Ding, Y., Wild, C., Shen, Q. & Zhou, J. Small molecule inhibitors targeting activator protein 1 (AP-1). *J. Med. Chem.* **57**, 6930–6948 (2014).
31. Yosef, R. et al. Directed elimination of senescent cells by inhibition of BCL-W and BCL-XL. *Nat. Commun.* **7**, 11190 (2016).
32. Levenson, J. D. et al. Exploiting selective BCL-2 family inhibitors to dissect cell survival dependencies and define improved strategies for cancer therapy. *Sci. Transl. Med.* **7**, 279ra40 (2015).
33. Liao, Y. R. & Lin, J. Y. Quercetin intraperitoneal administration ameliorates lipopolysaccharide-induced systemic inflammation in mice. *Life Sci.* **137**, 89–97 (2015).
34. Hickson, L. T. J. et al. Senolytics decrease senescent cells in humans: Preliminary report from a clinical trial of Dasatinib plus Quercetin in individuals with diabetic kidney disease. *EBioMedicine* **47**, 446–456 (2019).
35. Justice, J. N. et al. Senolytics in idiopathic pulmonary fibrosis: Results from a first-in-human, open-label, pilot study. *EBioMedicine* **40**, 554–563 (2019).
36. Sao, K. & Risbud, M. V. Sdc4 deletion perturbs intervertebral disc matrix homeostasis and promotes early osteopenia in the aging mouse spine. *Matrix Biol.* **131**, 46–61 (2024).
37. Tsingas, M. et al. Sox9 deletion causes severe intervertebral disc degeneration characterized by apoptosis, matrix remodeling, and compartment-specific transcriptomic changes. *Matrix Biol.* **94**, 110–133 (2020).
38. Kim, A. et al. Inhibition of EphA2 by Dasatinib Suppresses Radiation-Induced Intestinal Injury. *Int. J. Mol. Sci.* **21**, 9096 (2020).
39. Takasugi, M. et al. Small extracellular vesicles secreted from senescent cells promote cancer cell proliferation through EphA2. *Nat. Commun.* **8**, 15729 (2017).
40. Saul, D. et al. A new gene set identifies senescent cells and predicts senescence-associated pathways across tissues. *Nat. Commun.* **13**, 1–15 (2022).
41. Thompson, J. P. et al. Preliminary evaluation of a scheme for grading the gross morphology of the human intervertebral disc. *Spine (Philo. Pa 1976)* **15**, 411–415 (1990).
42. Novais, E. J. et al. Long-term treatment with senolytic drugs Dasatinib and Quercetin ameliorates age-dependent intervertebral disc degeneration in mice. *Nat. Commun.* **12**, 1–17 (2021).
43. Risbud, M. V. et al. Nucleus pulposus cells express HIF-1 α under normoxic culture conditions: A metabolic adaptation to the intervertebral disc microenvironment. *J. Cell Biochem* **98**, 152–159 (2006).
44. Levi, N., Papismadov, N., Solomonov, I., Sagi, I. & Krizhanovsky, V. The ECM path of senescence in aging: components and modifiers. *FEBS J.* **287**, 2636–2646 (2020).
45. van der Kraan, P. M. The changing role of TGF β in healthy, ageing and osteoarthritic joints. *Nat. Rev. Rheumatol.* **13**, 155–163 (2017).
46. Tessier, S. et al. Arp2/3 inactivation causes intervertebral disc and cartilage degeneration with dysregulated TonEBP-mediated osmoadaptation. *JCI Insight* **5**, e131382 (2020).
47. Sanborn, M. A., Wang, X., Gao, S., Dai, Y. & Rehman, J. Unveiling the cell-type-specific landscape of cellular senescence through single-cell transcriptomics using SenePy. *Nat. Commun.* **16**, 1884 (2025).
48. Vos, T. et al. Global, regional, and national incidence, prevalence, and years lived with disability for 301 acute and chronic diseases and injuries in 188 countries, 1990–2013: a systematic analysis for the Global Burden of Disease Study 2013. *Lancet* **386**, 743–800 (2015).
49. Makino, H. et al. A selective inhibition of c-Fos/activator protein-1 as a potential therapeutic target for intervertebral disc degeneration and associated pain. *Sci. Rep.* **7**, 16983 (2017).
50. Novais, E. J., Diekmann, B. O., Shapiro, I. M. & Risbud, M. V. p16INK4a deletion in cells of the intervertebral disc affects their matrix homeostasis and senescence associated secretory phenotype without altering onset of senescence. *Matrix Biol.* **82**, 54–70 (2019).
51. Diekmann, B. O. et al. Expression of p16INK4a is a biomarker of chondrocyte aging but does not cause osteoarthritis. *Aging Cell* **17**, e12771 (2018).
52. Zhu, Y. et al. The achilles' heel of senescent cells: From transcriptome to senolytic drugs. *Aging Cell* **14**, 644–658 (2015).
53. Sessions, G. A. et al. Controlled induction and targeted elimination of p16INK4a-expressing chondrocytes in cartilage explant culture. *FASEB J.* **33**, 12364–12373 (2019).
54. Lim, S. et al. Local delivery of senolytic drug inhibits intervertebral disc degeneration and restores intervertebral disc structure. *Adv. Healthc. Mater.* **11**, e2101483 (2022).
55. Carragee, E. J. et al. 2009 ISSLS Prize Winner: does discography cause accelerated progression of degeneration changes in the lumbar disc. *Spine (Philo. Pa 1976)* **34**, 2338–2345 (2009).
56. Paez-Ribes, M., González-Gualda, E., Doherty, G. J. & Muñoz-Espín, D. Targeting senescent cells in translational medicine. *EMBO Mol. Med.* **11**, e10234 (2019).
57. Mohanty, S., Pinelli, R., Pricop, P., Albert, T. J. & Dahia, C. L. Chondrocyte-like nested cells in the aged intervertebral disc are late-stage nucleus pulposus cells. *Aging Cell* **18**, e13006 (2019).
58. Beauséjour, C. M. et al. Reversal of human cellular senescence: Roles of the p53 and p16 pathways. *EMBO J.* **22**, 4212–4222 (2003).
59. Milanovic, M. et al. Senescence-associated reprogramming promotes cancer stemness. *Nature* **553**, 96–100 (2018).
60. Guo, Q. et al. STING promotes senescence, apoptosis, and extracellular matrix degradation in osteoarthritis via the NF- κ B signaling pathway. *Cell Death Dis.* **2021** 12:1 **12**, 1–14 (2021).
61. Kang, C. Senolytics and Senostatics: A Two-Pronged Approach to Target Cellular Senescence for Delaying Aging and Age-Related Diseases. *Mol. Cells* **42**, 821–827 (2019).
62. Ottone, O. K., Kim, C., Collins, J. A. & Risbud, M. V. The cGAS-STING Pathway Affects Vertebral Bone but Does Not Promote Intervertebral Disc Cell Senescence or Degeneration. *Front Immunol.* **13**, 882407 (2022).
63. Burt, K. G., Kim, M. K. M., Viola, D. C., Abraham, A. C. & Chahine, N. O. Nuclear factor κ B overactivation in the intervertebral disc leads to macrophage recruitment and severe disc degeneration. *Sci. Adv.* **10**, ead3194 (2024).
64. Mathas, S. Aberrantly expressed c-Jun and JunB are a hallmark of Hodgkin lymphoma cells, stimulate proliferation and synergize with NF- κ B. *EMBO J.* **21**, 4104–4113 (2002).
65. Spallarossa, P. et al. p38 MAPK and JNK Antagonistically Control Senescence and Cytoplasmic p16INK4A Expression in Doxorubicin-Treated Endothelial Progenitor Cells. *PLoS One* **5**, e15583 (2010).
66. Sundqvist, A. et al. JUNB governs a feed-forward network of TGF β signaling that aggravates breast cancer invasion. *Nucleic Acids Res.* **46**, 1180–1195 (2018).
67. Cui, L. et al. Activation of JUN in fibroblasts promotes pro-fibrotic programme and modulates protective immunity. *Nat. Commun.* **11**, 2795 (2020).
68. Choi, K. S. & Harfe, B. D. Hedgehog signaling is required for formation of the notochord sheath and patterning of nuclei pulposi within the intervertebral discs. *Proc. Natl. Acad. Sci. USA* **108**, 9484–9489 (2011).
69. Maeda, Y. et al. Indian Hedgehog produced by postnatal chondrocytes is essential for maintaining a growth plate and trabecular bone. *Proc. Natl. Acad. Sci. USA* **104**, 6382–6387 (2007).
70. Schindelein, J. et al. Fiji: An open-source platform for biological-image analysis. *Nat. Methods.* **9**, 676–682 (2012).
71. Mi, H. et al. Protocol Update for large-scale genome and gene function analysis with the PANTHER classification system (v.14.0). *Nat. Protoc.* **14**, 703–721 (2019).
72. Huang, X., Chen, C., Chen, Y., Xu, J. & Liu, L. Ormentin-1 alleviates interleukin-1 β (IL-1 β)-induced nucleus pulposus cells senescence. *Bioengineered* **13**, 13849–13859 (2022).
73. Purohit, A., Singh, A., Ghilchik, M. W., Serlupi-Crescenzi, O. & Reed, M. J. Inhibition of IL-6 + IL-6 soluble receptor-stimulated aromatase activity by the IL-6 antagonist, Sant 7, in breast tissue-derived fibroblasts. *Br. J. Cancer* **88**, 630–635 (2003).
74. Qiu, Y. et al. Combination of dasatinib and quercetin promotes osteogenic differentiation and stemness maintenance of hPDLSCs via YAP/TAZ. *Anim. Cells Syst. (Seoul.)* **29**, 201–211 (2025).
75. Gadecka, A. et al. The senolytic cocktail, dasatinib and quercetin, impacts the chromatin structure of both young and senescent vascular smooth muscle cells. *Geroscience* **47**, 3907–3925 (2025).
76. Aikawa, Y. et al. Treatment of arthritis with a selective inhibitor of c-Fos/activator protein-1. *Nat. Biotechnol.* **26**, 817–823 (2008).



Open Access This article is licensed under a Creative Commons Attribution 4.0 International License, which permits use, sharing, adaptation, distribution and reproduction in any medium or format, as long as you give appropriate credit to the original author(s) and the source, provide a link to the Creative Commons licence, and indicate if changes were made. The images or other third party material in this article are included in the article's Creative Commons licence, unless indicated otherwise in a credit line to the material. If material is not included in the article's Creative Commons licence and your intended use is not permitted by statutory regulation or exceeds the permitted use, you will need to obtain permission directly from the copyright holder. To view a copy of this licence, visit <http://creativecommons.org/licenses/by/4.0/>.

© The Author(s) 2026